Sheep-Wool-Fiber-Reinforced Rigid Polyurethane Composites: Comparative Effects of Alkaline, Oxidative, and APTES Treatments

Sergiu Lazăr[1], Dan Dobrotă[1,2,*], Florin Cristian Ciofu[1] and Augustin Stoica[1]

[1]*Lucian Blaga University of Sibiu, Faculty of Engineering, Department of Industrial Engineering and Management, Sibiu, Romania*

[2]*Academy of Romanian Scientists, Ilfov Street 3, 050045 Bucharest, Romania*

Abstract: Coarse sheep wool is a low-value byproduct whose use as reinforcement in rigid cast polyurethane remains less studied than its use in insulation products. This study compares untreated, alkaline-treated, oxidatively treated, and 3-aminopropyltriethoxysilane (APTES)-treated wool fibers in the same two-component polyurethane matrix (NEUKADUR MultiCast 1 / Hardener ISO 2, 100:100 by mass). Five series of twenty ASTM D638 Type I specimens were prepared: unreinforced polyurethane (P0) and four composites containing 10 wt% wool (approximately 8.0 vol%) cut to 10 ± 2 mm (T0-T3). Relative to P0, washed wool reduced tensile strength from 32.66 ± 0.59 to 26.00 ± 0.87 MPa and increased the apparent Young's modulus, determined from crosshead displacement, from 727 to 793 MPa. All treatments increased strength relative to T0, with the ranking T3 > T1 > T2 (Tukey HSD, adjusted $p < 0.001$). T3 reached 30.40 ± 0.68 MPa and had the highest apparent modulus (911 MPa) and the lowest 24 h water absorption among the reinforced series (1.24%). Density-derived porosity differed among series and covaried with strength; however, an exploratory covariance model retained a large series effect after adjustment. Because porosity was estimated indirectly and surface chemistry and fiber orientation were not measured directly, the results support an association between APTES treatment and improved composite performance but do not demonstrate a specific interfacial bonding mechanism or long-term moisture resistance. Under the tested formulation and processing conditions, APTES provided the best overall measured response, although none of the reinforced series recovered the tensile strength of the neat matrix.

Keywords: Sheep wool fiber, Rigid polyurethane, Surface treatment, APTES, Tensile properties, Density-derived porosity, Water absorption.

1. INTRODUCTION

Non-structural and semi-structural automotive components such as electronic control unit housings, covers, trim elements and sound- and heat-insulating parts are commonly produced from unreinforced engineering polymers or from short glass fiber composites. Replacing mineral or synthetic reinforcement in part with fibers of natural origin is one of the recurring directions of polymer ecodesign [1], motivated by the low density of the fiber, the renewable character of the resource, the reduced abrasion of processing equipment and the more favorable environmental balance of the reinforcement production stage [2, 3].

Within this landscape, coarse sheep wool occupies a particular position. It is a byproduct of ovine farming whose textile value is low and which, in many European regions, is effectively managed as waste, although its physical characteristics and protein composition recommend it as a raw material for composites [4, 5]. Wool has a reported thermal conductivity in the range 0.033–0.063 W/(m·K) [6] and a calorific value of about 19.5 MJ/kg [5], which explains why most of the applied literature has concentrated on thermal and acoustic insulation, on construction materials and, more recently, on energy recovery. Its use as an actual reinforcement in a rigid polymer matrix remains significantly less explored [7, 8].

The wool fiber consists mainly of keratin, a fibrillar protein stabilized by a dense network of disulfide bridges, hydrogen bonds, and ionic and hydrophobic interactions [9]. This architecture gives the fiber toughness and an elongation at break considerably larger than that of cellulosic fibers, but it also generates two difficulties specific to composites: the outer cuticle surface is covered by a covalently bound, strongly hydrophobic lipid layer that limits wetting by polar resins, and the inner cortex is hygroscopic, which introduces water into the system [7, 10, 11].

The second difficulty is critical when the matrix is a two-component polyurethane. Isocyanate groups react with water to form unstable carbamic acid, which decomposes into an amine and carbon dioxide; the amine in turn reacts with the remaining isocyanate, generating urea linkages. The practical consequences are parasitic isocyanate consumption, departure from the designed stoichiometry, and porosity in the cast part, a mechanism that can mask or even reverse the beneficial effect of reinforcement [12, 13]. The severity of the second consequence is documented for polyurethane systems in general: water acts as a

*Address correspondence to this author at the Lucian Blaga University of Sibiu, Faculty of Engineering, Department of Industrial Engineering and Management, Sibiu, Romania;
E-mail: dan.dobrota@ulbsibiu.ro

Received on 08-08-2026 Accepted on 12-09-2026 Published on 16-09-2026

E-ISSN: 2311-8717/26

chemical blowing agent, and lowering the isocyanate index from 1.1 to 0.7 has been shown to reduce compressive strength by about a third [14]. Any protocol for reinforcing a cast polyurethane with natural fibers must therefore treat fiber drying as a controlled process variable rather than as a routine preparatory step.

Chemical surface treatments are the usual route to improving the fiber–matrix interface in natural fiber composites. Three families are relevant for wool: alkaline treatment, which partly removes the lipid layer and exposes functional groups [15, 16]; oxidative treatment, which converts cuticle cystine into oxidized species, increasing surface polarity and wetting [17]; and silanization, which introduces a bifunctional molecular bridge between fiber and matrix [18-20]. Chemistry is not the only route to interface control. Geometric interlocking of the reinforcement raises local load transfer without altering surface chemistry, and in the same rigid polyurethane matrix used here it has been shown to retain 89.6 to 93.8% of the load capacity of integral reinforcement while using about 19% less fiber, with a functional performance ratio of 1.332 for the best interface geometry [21]. The two approaches address the same limitation from opposite directions, and the present work establishes what the chemical route alone can and cannot deliver in this matrix. Each of these also modifies the fiber itself, and in the case of keratin the sensitivity to alkaline media is well documented: the strength of the wool fiber decreases as the alkalinity of the medium into which it is introduced increases [6]. The trade-off between interface quality and reinforcement integrity is therefore the central question of this study.

A. Objective of the Study

The study investigates the effect of sheep wool fiber surface treatment on the tensile behavior of a rigid cast polyurethane matrix composite. The properties of the neat polyurethane are compared with those of a composite reinforced with untreated wool and with those of composites reinforced with alkaline-treated, oxidatively treated and aminosilane-treated fibers, at a constant fiber content of 10% by mass.

B. Research Question

How do NaOH, H_2O_2, and APTES treatments affect the tensile properties and 24 h water absorption of sheep-wool-fiber-reinforced rigid polyurethane under otherwise constant formulation and processing conditions?

C. Working Hypotheses

Three hypotheses were formulated as testable statements before data collection:

H1: introducing 10% wool by mass changes the tensile strength, stiffness and elongation at break of the material relative to the neat polyurethane.

H2: at least one of the three surface treatments raises the tensile strength of the composite above that of the untreated-fiber series.

H3: the APTES treatment yields the highest tensile strength among the reinforced series.

H1–H3 were stated on the basis of the existing literature and of plausible chemical mechanisms, and did not constitute confirmed results. The direction of the effect in H1 was deliberately left unspecified: at moderate volume fractions of short, discontinuous fibers, a decrease in strength relative to the unreinforced matrix is as possible an outcome as an increase. The ranking proposed in H3 was a prediction open to refutation. The decision rules used to declare each hypothesis supported are given in Section III-I.

D. Contribution of the Paper

To the authors' knowledge, the cited literature does not provide a side-by-side comparison of untreated, alkaline-treated, oxidatively treated, and APTES-treated sheep wool at constant fiber content in the same rigid cast polyurethane. Previous studies have mainly addressed wool in insulation materials, other polymer matrices, or one treatment route at a time. The present contribution is therefore a controlled comparative dataset linking tensile properties and 24 h water absorption with a density-derived estimate of porosity. The design is intentionally limited to one fiber content and does not directly measure interfacial chemistry, fiber orientation, or environmental impact; accordingly, the conclusions concern the relative performance of the five tested formulations rather than proof of a bonding mechanism or an ecodesign benefit.

2. STATE OF THE ART

A. Wool as a Reinforcement in Polymer Composites

Recent reviews of wool–polymer composites converge on one observation: wool brings clear advantages in damping, thermal and acoustic insulation and fire behavior, but its contribution to mechanical strength is modest and strongly dependent on interface quality [7, 8]. Patrucco *et al*. state the pattern in its sharpest form: incorporating wool into a polymer enhances the elastic modulus while simultaneously impairing tensile strength [23]. Mishra *et al*. show that keratin fibers act simultaneously as flame retardants and as reinforcements, the high nitrogen and sulfur content favoring the formation of a protective char layer [24]. Kulkarni *et al*. systematize

the uses of sheep wool as biomass in polymer composites and identify interfacial adhesion as the main technical limitation [4]. The systematic review by Ruiz-Díaz *et al*. on biocomposites reinforced with raw or minimally processed wool confirms the concentration of effort on thermal insulation applications and the relative absence of rigorously designed tensile studies [8]. The same group has since reported tensile, flexural, compressive and impact data for wool–epoxy composites, providing the closest published point of comparison for the present work [25].

The properties of the fiber itself are also variable. Starkova *et al*. show that the strength and elongation at break of sheep wool fibers follow statistical distributions sensitive to environmental conditions, which requires a sufficient number of replicates and an analysis of scatter rather than of means alone [10]. The same work provides the fiber properties used quantitatively in Section V-A: a tensile strength of 142.8 ± 30.3 MPa, a Young's modulus of 3.93 ± 0.61 GPa and a failure strain of 25.9 ± 11.4%, for a mean diameter of 37.4 ± 6.8 µm. Physico-chemical characterization of keratin extracted from wool and from feathers confirms the differences in composition and thermal stability between sources [26].

B. Wool–Polyurethane and Keratin–Polyurethane Composites

The number of studies devoted explicitly to keratin–polyurethane systems is small. Da Silva *et al*. developed a composite from dog wool microparticles in a polyurethane matrix intended for thermal insulation, demonstrating the processing compatibility of keratin with cast PUR systems [27]. Olszewski *et al*. studied bio-based polyurethane composites and hybrid composites with added natural and synthetic fibers, highlighting the sensitivity of mechanical properties to the content and surface state of the reinforcement [12]. Yuan *et al*. showed, for the wood fiber–polyurethane system, that water resistance and mechanical strength can be improved simultaneously through interface control [13]. These works support the feasibility of the approach but offer no direct comparison between surface treatments applied to wool in a rigid cast polyurethane matrix.

C. Alkaline Treatment

Alkaline treatment is the most frequently applied treatment for natural fibers. For lignocellulosic fibers it removes waxes, hemicelluloses and lignin, increases roughness and exposes hydroxyl groups available for bonding [15, 16]. For wool the mechanism differs: the alkaline medium attacks the cuticle lipid layer and, at high concentrations or long times, hydrolyzes peptide bonds and rearranges disulfide bridges, progressively degrading the fiber. Jóźwiak-Niedźwiedzka and Fantilli report, for wool-reinforced cementitious composites, that fiber strength is the better the lower the alkalinity of the matrix [6]. The existence of an optimum is visible in the composite data as well: for sugar palm fiber in thermoplastic polyurethane, Bachtiar *et al*. found the largest flexural gain at 2% NaOH, with the benefit falling away at 4% and 6% [28]. This is the direct justification for choosing a very low concentration of 0.1 M and a short contact time in the present protocol: the objective is surface cleaning, not mercerization.

D. Oxidative Treatment

Hydrogen peroxide treatment is used industrially to bleach wool. Wang *et al*. showed that treating wool fabric with H_2O_2 modifies the surface properties of the fiber, oxidation of sulfur-containing groups increasing surface hydrophilicity and reactivity [17]. From a composite perspective, controlled oxidation offers an interesting compromise: it raises surface polarity and wetting without the hydrolytic attack characteristic of alkaline media. Braniša *et al*. discuss several selective modifications of sheep wool oriented toward non-textile applications, including oxidative treatments, stressing that treatment intensity determines whether the net effect is functionalization or degradation [11]. The composite-level evidence is more reserved: Flores *et al*. compared NaOH, hydrogen peroxide and peracetic acid on jute–polyester laminates and found gains in flexural and short-beam strength but no significant change in tensile properties [29].

E. Silanization and Aminosilane Coupling Agents

Bifunctional silanes are widely used as coupling agents in natural-fiber composites. Hydrolysis of their alkoxy groups produces silanols that can condense with reactive groups at a fiber surface, while the organofunctional group can interact with the matrix [20]. For polyurethane systems, the primary amino group of APTES may react with isocyanate groups and form urea linkages. This reaction provides a plausible route to stronger interfacial coupling, but its occurrence on the treated wool in the present study was not verified directly.

Application of silanes to wool has been demonstrated experimentally. Conzatti *et al*. functionalized wool fibers with a silane-based coupling agent for polypropylene composites, obtaining improved fiber–matrix compatibility [18]. Pawlak *et al*. used silanized wool fibers from dairy industry waste for plasticized PLA composites intended for injection molding [19]. Both studies confirm that a keratin

surface can be silanized effectively, although the anchoring mechanism differs from that of cellulosic fibers, also involving the amino, hydroxyl and carboxyl groups of the protein chains. For cellulosic systems the quantitative benefit is well established: Alao *et al*. report that alkali pretreatment of hemp raised the tensile strength of a PLA composite by 14%, and that a subsequent silane step added a further 10%, for a total of 29% over untreated fiber [30].

F. Interface and Moisture Uptake

Water uptake can affect the dimensional stability and long-term mechanical behavior of natural-fiber composites [2]. Wool is hygroscopic, and oxidative treatments that increase surface polarity may also increase short-term water absorption. Pavlovic *et al*. report 24 h uptake values of approximately 0.7-2% for natural-fiber composites and strength losses after prolonged moisture exposure [31]. The present 24 h immersion test is therefore used as a comparative screening measure; it is not treated as proof of long-term moisture resistance or durability.

G. Identified Gap

The reviewed studies document the three treatment routes individually, but a controlled comparison within one rigid polyurethane matrix and at one wool content is missing. Casting-related voids are an additional concern in isocyanate-cured systems because residual moisture can generate carbon dioxide. This study addresses that gap by comparing the tensile response and 24 h water absorption of the four fiber surface states and by reporting density-derived porosity alongside the mechanical results. Because the porosity measure is indirect and the treatments were not verified spectroscopically, the analysis distinguishes measured outcomes from mechanistic interpretations.

3. MATERIALS AND METHODS

A. The Polyurethane Matrix

The matrix was the two-component cast polyurethane system NEUKADUR MultiCast 1 with NEUKADUR Hardener ISO 2. The manufacturer's catalogue data are reproduced in Table **1** [32]. The system has a mixing ratio of 100:100 parts by mass, that is 1:1, and a very low viscosity of both components, which makes it suitable for gravity casting into silicone molds but imposes a very short working time.

The tensile strength declared by the manufacturer, about 33 MPa, is reported according to DIN 53455, a German standard that has been withdrawn and replaced in current practice by the DIN EN ISO 527 series. Catalogue values are therefore treated in this study purely as an indicative reference; the effective comparison value for series P0 is the one measured experimentally according to ASTM D638 [33].

Table 1: Properties of the NEUKADUR MultiCast 1 / Hardener ISO 2 polyurethane system (catalogue data) [32]

Property	Value	Standard
Mixing ratio (by mass)	100 : 100	—
Density MultiCast 1 (20 °C)	0.95 g/cm³	—
Density Hardener ISO 2 (20 °C)	1.10 g/cm³	—
Density of the mixture (calculated)	1.02 g/cm³	—
Viscosity MultiCast 1 (20 °C)	35 mPa·s	—
Viscosity Hardener ISO 2 (20 °C)	75 mPa·s	—
Working time (100 g, 20 °C)	3.5 min	—
Demolding (4–5 mm, 25 °C)	75 min	—
Shore D hardness	75	DIN 53505
Tensile strength	33 MPa	DIN 53455
Elongation at break	6 %	DIN 53455
Flexural strength	33 MPa	DIN 53452
Flexural modulus	650 MPa	DIN 53457

The density of the mixture was calculated from the component densities at a 1:1 mass ratio.

No filler B or other additives were used, in order not to introduce an additional variable. The polyol-to-isocyanate ratio was unchanged in all series: the fiber was added as a supplementary phase, not as a substitute for a reactive component.

B. The Reinforcement

The reinforcement was Țurcană sheep wool from a coarse-wool Romanian breed. The fleece was obtained by routine annual shearing from a single flock in Gorj County, Romania, and was used as a low-value agricultural byproduct rather than as a textile-grade feedstock. Fiber diameters were in the range 30-40 μm, consistent with the mean value reported for sheep wool by Starkova *et al*. [10]. The raw fibers were cut to 10 ± 2 mm before the common washing step and were incorporated at 10% of the total composite mass.

A density of 1.31 g/cm³ was adopted for the wool fiber. With an unfilled matrix density of 1.02 g/cm³, the corresponding fiber volume fraction is 8.0%, calculated as:

$$V_f = (w_f / \rho_f) / (w_f / \rho_f + w_m / \rho_m) \quad (1)$$

where wf and wm are the mass fractions of fiber and matrix and ρf and ρm are their respective densities. Thus, 10 wt% wool corresponds to approximately 8.0 vol% for the densities adopted in this work.

The fiber density was not measured in the present work, and it enters the theoretical composite density and therefore the porosity estimate of Section III-H. Rather than treat it as exact, its influence was bounded: adopting 1.28 g/cm³ instead of 1.31 g/cm³ shifts the estimated porosity of every reinforced series by approximately 0.2 percentage points in the same direction, leaving the ranking between series and every conclusion drawn from it unchanged. Removing the assumption entirely would require helium pycnometry on the treated fibers, which is listed among the characterizations recommended in Section V-F.

C. Experimental Series and Treatments

Five series were prepared, with twenty tensile specimens per series (100 specimens in total). The wool was first cut to 10 ± 2 mm, washed with neutral detergent and distilled water, rinsed, and dried. The washed reference lot was designated T0. Separate aliquots were then subjected to alkaline treatment (T1), oxidative treatment (T2), or APTES treatment (T3) under the conditions in Table **2**. After the treatment-specific rinsing step, all reinforced lots underwent the same final drying schedule (60 °C for 12 h followed by 80 °C for 2 h) and were stored in a desiccator until mixing. This sequence separates the common cleaning and final drying steps from the treatment-specific operations.

Table 2: Experimental series and surface treatment parameters

Series	Treatment	Parameters
P0	— (matrix)	Unreinforced polyurethane, no fibers
T0	Washing	Neutral detergent + distilled water, rinsing, drying
T1	Alkaline	NaOH 0.1 M, 30 min, room temperature, rinsing to pH 6–7
T2	Oxidative	H_2O_2 6%, 60 min, room temperature, rinsing to pH 6-7
T3	Aminosilane	APTES 1% v/v in ethanol/water 95:5, pH ≈ 4.5 (acetic acid); hydrolysis 30 min, fiber contact 60 min, rapid ethanol rinse

All reinforced series contained 10 wt% wool, calculated relative to the total composite mass, with fibers cut to 10 ± 2 mm; n = 20 tensile specimens per series. The polyurethane components remained at a 1:1 mass ratio. Common final drying: 60 °C for 12 h + 80 °C for 2 h, followed by desiccator storage.

The parameters were deliberately chosen in the mild range. The NaOH concentration of 0.1 M and the time of 30 minutes at room temperature aimed at removing the lipid layer without degrading the keratin, consistent with the documented sensitivity of wool to alkaline media [6]. The H_2O_2 concentration of 6% and the time of 60 minutes correspond to moderate oxidation, below typical industrial bleaching conditions [17]. The APTES solution, 1% v/v in ethanol/water 95:5 adjusted to pH ≈ 4.5 with acetic acid, follows standard alkoxysilane prehydrolysis practice: the weakly acidic medium catalyzes hydrolysis and slows silanol self-condensation, favoring deposition of a thin layer rather than polysiloxane agglomerates [20].

D. Fiber Drying and Moisture Control

After the treatment-specific rinsing step, each fiber lot was dried at 60 °C for 12 h and then at 80 °C for 2 h, followed by storage in a desiccator until mixing. Constant mass was verified gravimetrically for each lot before use. The same schedule was applied to T0 after washing and to T1-T3 after treatment so that drying history was controlled across the reinforced series.

$$R–NCO + H_2O \rightarrow [R–NH–COOH] \rightarrow R–NH_2 + CO_2\uparrow \quad (2)$$

$$R–NH_2 + R'–NCO \rightarrow R–NH–CO–NH–R' \quad (3)$$

Reaction (2) consumes isocyanate and releases carbon dioxide, which can form voids during curing; reaction (3) forms urea linkages and alters the local network. Controlling the final drying schedule was therefore necessary to reduce moisture-related variation among fiber lots. Residual moisture was not measured instrumentally, so the constant-mass check should be understood as a processing control rather than a direct moisture-content determination.

E. Specimen Geometry

ASTM D638 Type I specimens were used [33], with the dimensions given in Table **3** and in Figure **1**.

Table 3: Geometry of the ASTM D638 Type I specimen used [33]

Parameter	Symbol	Value
Overall length	L	165 mm
Overall width	W	19 mm
Length of narrow section	L_n	57 mm
Width of narrow section	W_n	13 mm
Fillet radius	R	76 mm
Gauge length	L_0	50 mm
Thickness	t	4.0 mm
Narrow section area	A	52 mm²
Planar contour area	A_p	26.23 cm²
Specimen volume	V	10.49 cm³

The planar area was obtained by integrating the contour profile; the volume corresponds to a thickness of 4.0 mm.

The planar contour area of the specimen, calculated by integrating the profile formed by the two grip sections, the two fillets of radius 76 mm and the narrow

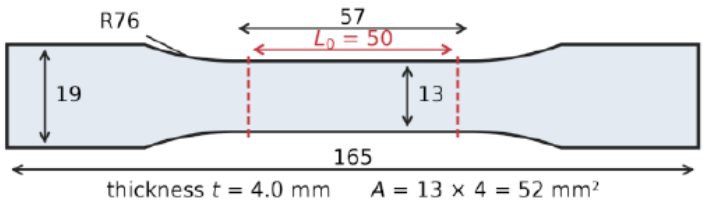

Figure 1: Geometry of the ASTM D638 Type I specimen used in the study; dimensions in millimeters.

section, is 26.23 cm². For a thickness of 4.0 mm this gives a volume of 10.49 cm³ per specimen. These values underlie the mass balance of the following section.

F. Mass Balance

The density of the unfilled mixture, calculated from the component densities at a 1:1 mass ratio, is 1.02 g/cm³. The density of the composite with 10% wool by mass, obtained from the inverse rule of mixtures, is 1.043 g/cm³, giving a nominal mass of 10.94 g for a 4 mm specimen. The breakdown by component and the quantities required for a complete series of 20 tensile specimens are given in Table **4**. A 15% surplus was applied to cover losses on mixing, adhesion to the vessel walls and casting. The resulting quantities exceed the capacity of a single batch, given the working time of 3.5 minutes; each series was therefore cast in successive batches of five specimens.

Table 4: Mass balance for one reinforced series (10% wool by mass, 20 specimens)

Component	One specimen	20 specimens + 15%
Wool fiber	1.09 g	25.17 g
NEUKADUR MultiCast 1	4.92 g	113.25 g
NEUKADUR Hardener ISO 2	4.92 g	113.25 g
Total	10.94 g	251.67 g

Calculated for a volume of 10.49 cm³ and a composite density of 1.043 g/cm³ (ρ fiber = 1.31 g/cm³, ρ matrix = 1.02 g/cm³), corresponding to a fiber volume fraction of 8.0%.

For series P0, without fibers, the nominal specimen mass is 10.70 g, corresponding to a volume of 10.49 cm³ at a density of 1.02 g/cm³, split equally between the two components; for 20 specimens with a 15% surplus this gives 245.97 g of mixture. The specimens used for water absorption, described in Section III-H, were cast separately from the same formulations and are additional to the quantities in Table **4**; the material required for them was calculated on the same basis.

G. Composite Preparation

For each reinforced batch, the weighed fiber fraction was dispersed in the MultiCast 1 component before the hardener was introduced. Slow stirring was continued until the distribution appeared visually homogeneous and visible agglomerates were broken up. Hardener ISO 2 was then added at a MultiCast 1:Hardener mass ratio of 1:1. Because wool represented 10 wt% of the final composite, the nominal formulation was 10 wt% wool, 45 wt% MultiCast 1, and 45 wt% Hardener ISO 2. The mixture was homogenized rapidly and gravity-cast into dry silicone molds. Each series was produced in successive batches of five specimens to remain within the approximately 3.5 min working time.

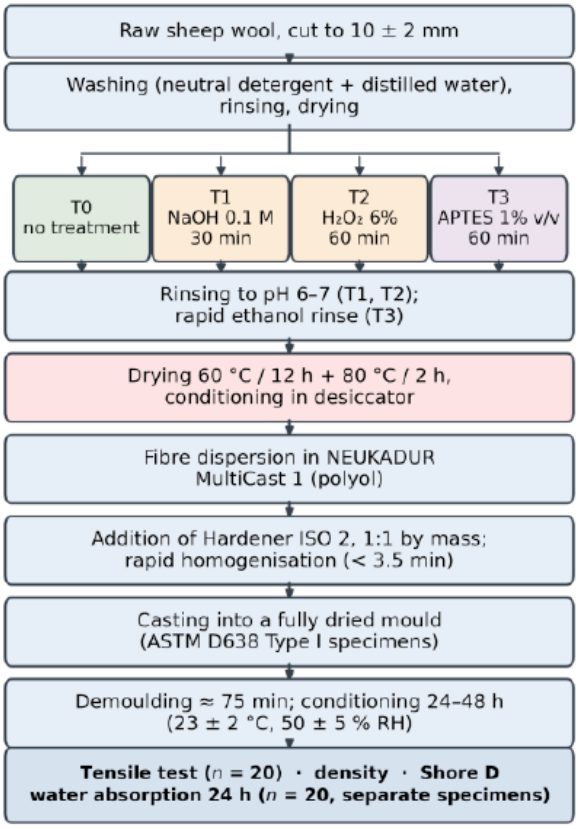

Figure 2: Experimental flow, from raw wool to the characterization of the five series.

Specimens were demolded after about 75 minutes, corresponding to a thickness of 4–5 mm at 25 °C, and conditioned for 24 to 48 hours at 23 ± 2 °C and 50 ± 5% relative humidity before testing. For each casting the ambient temperature, the relative humidity, the actual weighed masses of the three components and any

visually observed deviations such as air bubbles or fiber-rich zones were recorded.

H. Characterization

1) Tensile testing: tests were conducted on ASTM D638 Type I specimens [33] using a Sauter TVM 20KN120N motorized vertical test stand (Sauter GmbH / KERN & SOHN GmbH, Balingen, Germany) fitted with a force gauge. A constant crosshead speed of 5 mm/min was applied to all five series. Tensile strength was calculated from the maximum force and the nominal narrow-section area of 52 mm².

$$A = 13\ \text{mm} \times 4\ \text{mm} = 52\ \text{mm}^2 \quad (4)$$

and the tensile strength was calculated as:

$$\sigma = F_{max} / A \quad (5)$$

The measured strength range of 26-33 MPa corresponds to breaking forces of approximately 1.35-1.70 kN, within the measurement range used for all series.

2) Apparent Young's modulus: calculated as a chord modulus between two preset strain values on the initial linear portion of the curve, using the same interval for all series:

$$E = (\sigma_2 - \sigma_1) / (\varepsilon_2 - \varepsilon_1) \quad (6)$$

Force and displacement were recorded by the test-stand measuring system. Strain was derived from crosshead displacement over the nominal gauge length; no clip-on extensometer was used. The reported values are therefore apparent Young's moduli and apparent elongations that include machine and grip compliance. They are suitable for comparison among series tested on the same setup, but they should not be treated as extensometer-based design values.

3) Apparent elongation at break: calculated from crosshead displacement at maximum force relative to the nominal gauge length and recorded to a resolution of 0.1%. Comparisons among reinforced series are interpreted cautiously because this resolution is similar to their within-series standard deviations.

4) Density and apparent porosity: density was determined by the ASTM D792 displacement method [34]. The relative difference between the measured density and the theoretical density calculated at the nominal formulation was used as a density-derived porosity estimate. Because local fiber-content variation also affects density, this value is an indirect proxy for void content rather than a direct void measurement.

5) Shore D hardness: measured according to ASTM D2240 [35] on each specimen, away from the edges. One value per specimen is reported and the series statistics are computed over the twenty specimens.

6) Water absorption at 24 h: determined according to ASTM D570 [36], on twenty specimens per series cast separately from those subjected to tensile testing, as:

$$WA = 100 \cdot (m_2 - m_1) / m_1 \quad (7)$$

where m_1 is the mass of the dried and conditioned specimen and m_2 the mass after 24 hours of immersion.

I. Statistical Analysis

Twenty specimens were tested per series. Results are reported as mean ± sample standard deviation, together with the coefficient of variation (CV) and 95% confidence intervals for the mean:

$$CV = 100 \cdot s / \bar{x} \quad (8)$$

Series effects were evaluated at $\alpha = 0.05$. Shapiro-Wilk tests within series and the median-centered Levene test were used to assess the assumptions for one-way ANOVA. When assumptions were adequate, ANOVA was followed by Tukey HSD comparisons. When variance homogeneity was rejected, the Alexander-Govern test and Games-Howell comparisons were used. Kruskal-Wallis results were retained as a sensitivity check but were not used as a second decision rule.

For tensile strength and apparent modulus, effect size was summarized by η^2 and pairwise differences were reported with adjusted p values and 95% confidence intervals. For outcomes analyzed by Alexander-Govern, η^2 was not interpreted as an effect size for that test.

The association between density-derived porosity and tensile strength was examined both across and within the reinforced series. An analysis of covariance (ANCOVA) included series as a factor and the per-specimen porosity estimate as a covariate after testing the series-by-porosity interaction. Because the porosity estimate is indirect, this model is interpreted as an adjustment and not as evidence of causality.

A two-parameter Weibull distribution was fitted to tensile strength by maximum likelihood. The shape parameter m, characteristic strength σ0, B10, and B1 are reported descriptively; bootstrap confidence intervals were calculated for m. Given n = 20 per series, the lower-tail estimates are used to compare the

present series and are not presented as production allowables.

The pre-specified hypotheses were assessed from the adjusted pairwise tensile-strength comparisons: H1 required a significant difference between P0 and T0, H2 required at least one treated series to exceed T0, and H3 required T3 to exceed every other reinforced series.

4. RESULTS

A. Descriptive Statistics

The tensile test results are given in Table **5** and the complementary physical properties in Table **6**. All 100 specimens failed within the narrow section; no specimen was excluded.

Table 5: Tensile Test Results (n = 20 per series)

Series	σ_t ± SD (MPa)	CV (%)	E ± SD (MPa)	ε_r ± SD (%)
P0	32.66 ± 0.59	1.81	727 ± 13	5.76 ± 0.12
T0	26.00 ± 0.87	3.35	793 ± 17	4.14 ± 0.12
T1	28.42 ± 0.62	2.18	849 ± 13	4.08 ± 0.07
T2	27.22 ± 0.76	2.79	825 ± 11	3.95 ± 0.12
T3	30.40 ± 0.68	2.24	911 ± 14	4.23 ± 0.09

σt - tensile strength; E - apparent Young's modulus based on crosshead displacement; εr - apparent elongation at break; CV - coefficient of variation of tensile strength.

Table 6: Complementary Physical Properties (n = 20 per series)

Series	ρ (g/cm³)	Porosity (%)	Shore D	WA_{24} (%)
P0	1.016 ± 0.006	0.34 ± 0.60	75.0 ± 0.8	0.32 ± 0.04
T0	0.992 ± 0.010	4.88 ± 0.95	75.8 ± 0.9	1.68 ± 0.16
T1	1.010 ± 0.008	3.17 ± 0.77	76.8 ± 0.7	1.84 ± 0.19
T2	0.999 ± 0.009	4.21 ± 0.86	76.5 ± 0.8	2.31 ± 0.22
T3	1.019 ± 0.007	2.30 ± 0.67	77.6 ± 0.6	1.24 ± 0.13

Porosity is the relative difference between the theoretical density and the density measured according to ASTM D792; it is computed for each specimen from its own measured density and the theoretical density of its series. WA_{24} – water absorption at 24 h, ASTM D570, on separate specimens.

Tensile strength decreases from 32.66 MPa for the unreinforced matrix to 26.00 MPa for the composite with untreated fibers, a loss of 20.4%. The three treatments recover part of this loss, in the order T3 > T1 > T2. The graphical representation, with 95% confidence intervals and Tukey significance groups, is given in Figure **3**.

The apparent modulus was higher for all reinforced series than for P0 and reached its largest mean in T3 (911 MPa). Apparent elongation at break decreased from 5.76% for P0 to 3.95-4.23% for the reinforced series. These deformation-based quantities were derived from crosshead displacement and are therefore comparative rather than extensometer-based material properties.

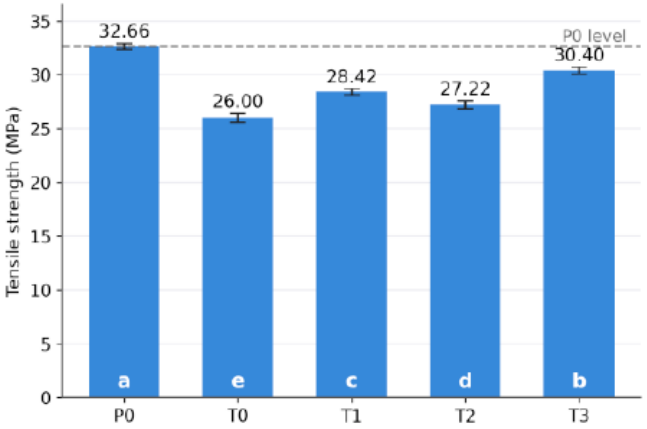

Figure 3: Tensile strength by series; error bars = 95% confidence interval of the mean; letters indicate Tukey significance groups (different letters = significant difference at α = 0.05); the dashed line marks the level of the unreinforced matrix.

B. Verification of Statistical Assumptions

Before applying the analysis of variance, normality of residuals was checked by the Shapiro–Wilk test applied to each series, and homogeneity of variances by the Levene test with median centering. The results are summarized in Table **7**.

Table 7: Verification of the Parametric Test Assumptions

Quantity	Shapiro–Wilk (min p)	Levene (p)	Procedure adopted
σ_t	0.047 (T2)	0.473	One-way ANOVA
E	0.427 (P0)	0.660	One-way ANOVA
ε_r	0.001 (T3)	0.023	Alexander–Govern
WA_{24}	0.140 (T3)	< 0.001	Alexander–Govern

Shapiro–Wilk applied to each series; the smallest p value and the corresponding series are reported. Levene with median centering. For WA_{24} the homogeneity assumption is rejected, so classical ANOVA does not apply.

For tensile strength and apparent modulus, the equal group sizes and the absence of variance heterogeneity supported the ANOVA route. The isolated Shapiro-Wilk result for T2 strength (p = 0.047) was treated as a minor departure; the Kruskal-Wallis sensitivity analysis led to the same overall conclusion.

Apparent elongation at break failed the normality and homogeneity checks. Because the 0.1% recording resolution produced only a few distinct values within each series, Alexander-Govern and Games-Howell results are reported, and small differences among reinforced series are considered resolution-limited.

For 24 h water absorption, Levene's test rejected variance homogeneity ($p < 0.001$); therefore, the Alexander-Govern test and Games-Howell comparisons were used. The Kruskal-Wallis sensitivity analysis agreed with the omnibus result.

C. Analysis of Variance and Pairwise Comparisons

The summary of the analysis of variance for the four quantities is given in Table **8**. The factor is the fiber surface state, with five levels.

Table 8: Summary of Omnibus Statistical Tests

Quantity	Test	Statistic	p	η^2
σ_t	ANOVA	$F(4, 95) = 274.75$	< 0.001	0.920
E	ANOVA	$F(4, 95) = 492.59$	< 0.001	0.954
ε_r	Alexander–Govern	$\chi^2(4) = 221.77$	< 0.001	—
WA_{24}	Alexander–Govern	$\chi^2(4) = 356.87$	< 0.001	—

Factor: fiber surface state (5 levels). η^2 is reported only for the ANOVA outcomes (tensile strength and apparent modulus). Alexander-Govern outcomes are accompanied by the test statistic and p value without interpreting η^2 as variance explained.

The series effect was significant for tensile strength ($F(4, 95) = 274.75$, $p < 0.001$, $\eta^2 = 0.920$) and apparent modulus ($F(4, 95) = 492.59$, $p < 0.001$, $\eta^2 = 0.954$). The Alexander-Govern tests were also significant for apparent elongation and 24 h water absorption ($p < 0.001$), but no variance-explained interpretation is assigned to those statistics.

Table 9: Tukey HSD Pairwise Comparisons for Tensile Strength

Pair	Δσ (MPa)	95% CI	Adjusted p
P0 − T0	+6.66	[6.03; 7.28]	< 0.001
P0 − T1	+4.24	[3.61; 4.87]	< 0.001
P0 − T2	+5.44	[4.81; 6.07]	< 0.001
P0 − T3	+2.26	[1.63; 2.89]	< 0.001
T0 − T1	−2.42	[−3.04; −1.79]	< 0.001
T0 − T2	−1.22	[−1.84; −0.59]	< 0.001
T0 − T3	−4.40	[−5.02; −3.77]	< 0.001
T1 − T2	+1.20	[0.57; 1.83]	< 0.001
T1 − T3	−1.98	[−2.61; −1.35]	< 0.001
T2 − T3	−3.18	[−3.81; −2.55]	< 0.001

Δσ is the difference between the mean of the first series and that of the second. All ten pairs are significant at $\alpha = 0.05$.

All tensile-strength pairs differed significantly after Tukey adjustment, giving the observed order P0 > T3 > T1 > T2 > T0. For apparent elongation, Games-Howell comparisons found no detectable difference for T0 versus T1 ($p = 0.443$) or T0 versus T3 ($p = 0.118$); other small contrasts among reinforced series remain limited by the 0.1% measurement resolution.

D. Weibull Analysis and Lower-Tail Strength

A two-parameter Weibull model was used to describe the tensile-strength distributions and their lower tails. Table **10** reports the fitted shape parameter, characteristic strength, B10, and B1 for comparison among the five series.

T3 had higher fitted B10 and B1 values than the other reinforced series, consistent with its higher mean strength. Because each fit is based on twenty specimens from one wool lot and one processing campaign, the Weibull parameters describe within-study repeatability and should not be treated as population-wide reliability or design allowables.

E. Water Absorption: Pairwise Comparisons

Because the homogeneity of variances is rejected for water absorption, the pairwise comparisons were made with the Games–Howell procedure, which uses Welch degrees of freedom for each pair. Nine of the ten pairs differ at $p < 0.001$. The exception is T0 versus T1, where the difference of 0.16 percentage points gives $p = 0.050$ and does not reach significance. The alkaline treatment therefore does not measurably change water uptake relative to the untreated fiber, and the hierarchy of water absorption is properly stated as T2 > T1 ≈ T0 > T3 > P0.

Table 10: Weibull Parameters and Lower-Tail Strengths for the Five Series

Series	m [95% CI]	σ_0 (MPa)	B10 (MPa)	B1 (MPa)	R^2
P0	67.4 [54.6; 96.2]	32.93	31.85	30.76	0.959
T0	35.8 [28.2; 54.0]	26.40	24.79	23.22	0.982
T1	44.7 [35.8; 84.8]	28.72	27.32	25.92	0.927
T2	32.5 [27.9; 55.6]	27.61	25.76	23.97	0.790
T3	49.5 [42.0; 66.9]	30.73	29.36	28.00	0.936

m – Weibull shape parameter, by maximum likelihood, with a bootstrap confidence interval; σ_0 – characteristic strength; B10 and B1 – strengths below which 10% and 1% of specimens fall; R^2 – coefficient of determination of the Weibull probability plot.

F. Porosity, Treatment, and the Direction of their Relationship

Density-derived porosity differed among the reinforced series ($F(3, 76) = 38.68$, $p < 0.001$), with means of 4.88% for T0, 4.21% for T2, 3.17% for T1, and 2.30% for T3. Across the four series means, lower estimated porosity coincided with higher strength ($r = -0.991$). A pooled regression over the 80 reinforced specimens gave a slope of -0.87 MPa per percentage point and $R^2 = 0.385$; this aggregate association cannot distinguish formulation from porosity effects.

Within the individual series, slopes were positive (+0.18 to +0.37 MPa per percentage point) and none was individually significant. This reversal relative to the pooled slope indicates strong between-series structure, but it should not be interpreted as evidence that voids improve strength because the density-derived estimate can also reflect local fiber-content variation.

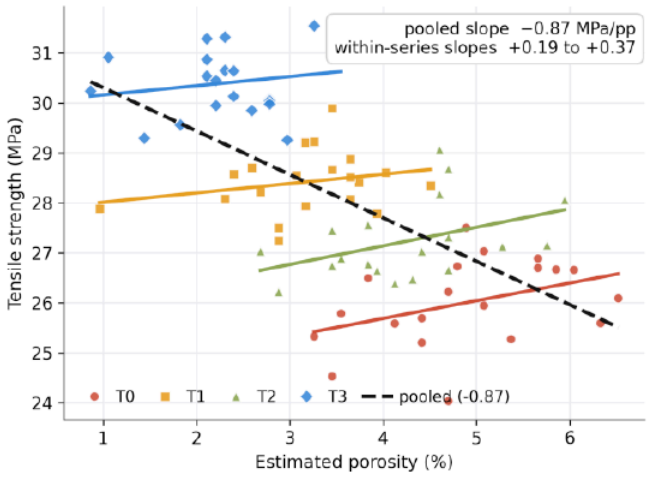

Figure 4: Tensile strength against estimated porosity for the 80 reinforced specimens. Solid lines are the regressions fitted within each series; the dashed line is the regression pooled over all four. The pooled slope is negative while every within-series slope is positive, so the aggregate relationship does not describe the behavior of any individual series.

The series-by-porosity interaction was not significant ($F(3, 72) = 0.25$, $p = 0.862$), so an additive ANCOVA was fitted. The series term remained significant after adjustment ($F(3, 75) = 79.50$, $p < 0.001$; partial $\eta^2 = 0.740$), while the porosity covariate had partial $\eta^2 = 0.028$ ($p = 0.0038$). Adjusted contrasts against T0 were +2.92 MPa for T1, +1.42 MPa for T2, and +5.16 MPa for T3.

These results show that the treatment-series differences persist after statistical adjustment for the density-derived porosity measure. They do not establish that the differences are independent of true void content, because voids were not measured directly and the covariate is partly sensitive to local fiber content.

G. Complementary Properties

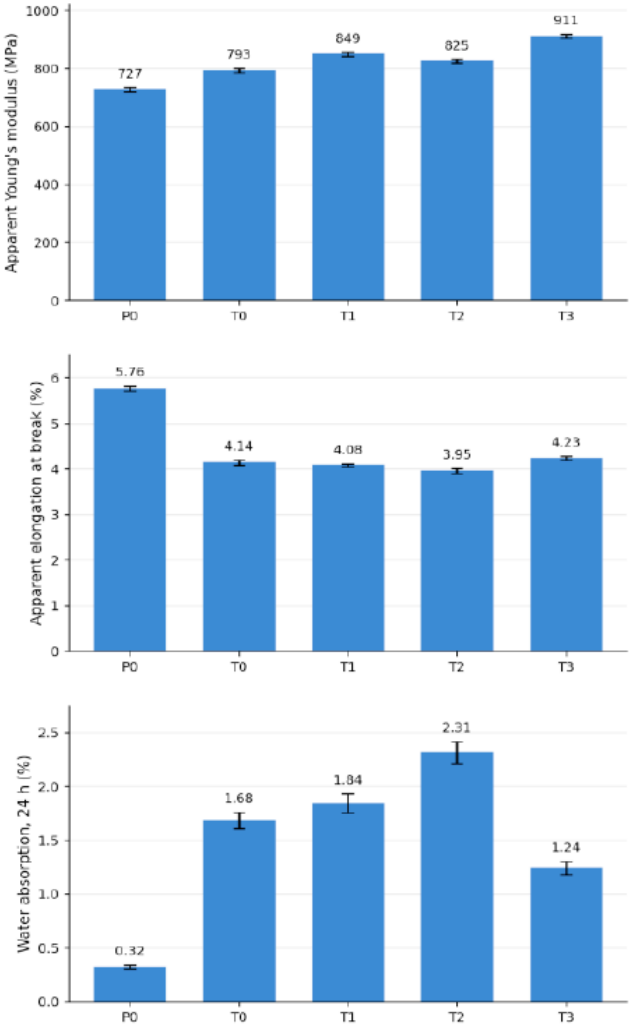

Figure 5: Apparent Young's modulus, apparent elongation at break, and 24 h water absorption by series; error bars show 95% confidence intervals of the mean.

Water absorption after 24 h increased from 0.32% for P0 to 1.24-2.31% for the reinforced series. T2 had the highest value and T3 the lowest value among the composites. These results compare short-term uptake only; no conclusion is drawn about long-term moisture resistance or retention of mechanical properties after conditioning.

H. Hypothesis Testing

H1 was supported: relative to P0, T0 showed lower tensile strength and apparent elongation and a higher apparent modulus ($p < 0.001$). H2 was supported because all three treated series exceeded T0 in tensile strength (adjusted $p < 0.001$). H3 was supported within the tested formulations: T3 exceeded T1, T2, and T0, but remained 2.26 MPa (6.9%) below P0. Thus, APTES produced the highest reinforced-series strength without restoring the neat-matrix value.

5. DISCUSSION

A. Why Reinforcement Lowers the Strength

The loss of strength on introducing the untreated fiber is not an unexpected result, but the mechanism usually invoked for short-fiber composites does not apply here, and it is worth establishing that before proposing an alternative.

The classical explanation is that fibers shorter than the critical length cannot be loaded to their strength and act as discontinuities. The critical length follows from the Kelly–Tyson relation, $l_c = \sigma_f \cdot d/(2\tau)$, where σ_f is the fiber strength, d the fiber diameter and τ the interfacial shear strength. Taking σ_f = 142.8 MPa, the value measured on sheep wool fibers by Starkova *et al*. [10], and the 30–40 μm diameter range of the fibers used here, Table **11** evaluates it against the range of interfacial shear strengths physically available to this system.

Table 11: Critical Fiber Length from the Kelly–Tyson Relation, for σ_f = 142.8 MPa [10]

d (μm)	τ (MPa)	l_c (mm)	l / l_c
30	10	0.21	47
30	5	0.43	23
40	10	0.29	35
40	5	0.57	18
40	2	1.43	7

l = 10 mm is the nominal cut length. Values are model estimates based on literature fiber strength and assumed interfacial shear strength.

Across the assumed interfacial shear-strength range of 2-10 MPa, the calculated critical length is 0.21-1.43 mm, so the nominal 10 mm fibers are 7-47 times longer than the modeled critical length. This calculation makes insufficient fiber length an unlikely sole explanation for the strength loss, but it remains sensitive to literature-derived fiber strength and assumed interfacial shear strength.

The apparent stiffness data were also explored with a Krenchel-type rule of mixtures, Ec = η·Ef·Vf + Em·Vm, using Ef = 3.93 GPa from Starkova *et al*. [10]. The resulting η values are reported as apparent efficiency factors because they combine orientation, interfacial load transfer, porosity, and uncertainty arising from crosshead-based strain measurement.

The calculated pore-adjusted factors of 0.66-0.91 are higher than reference values for idealized random orientation. This is consistent with preferential in-plane and flow-direction alignment in a 4 mm thick dog-bone cavity, but it does not constitute a direct orientation measurement. Image analysis or micro-computed tomography would be required to separate alignment from the other contributions embedded in η.

Table 12: Apparent Krenchel Efficiency Factors Calculated from the Measured Stiffness (Ef = 3.93 GPa [10], Vf = 0.0796, Em = 727 MPa)

Series	E (MPa)	η, as measured	η, pore-free basis
T0	793	0.40	0.66
T1	849	0.57	0.76
T2	825	0.50	0.74
T3	911	0.77	0.91

Reference values for idealized orientation states are shown for context. The calculated η values also include effects of interface, porosity, and crosshead-based strain measurement and are not direct measurements of orientation.

Taken together, the estimates suggest that the strength reduction is more plausibly associated with several concurrent factors than with fiber length alone: higher void content in the reinforced castings, local strain concentrations near fiber ends or debonded regions, and limited load transfer at the wool-polyurethane interface. The decrease in apparent elongation from 5.76% to approximately 4% is consistent with earlier composite failure, although fracture-surface microscopy would be needed to identify the dominant failure mechanism.

B. Ranking of the Treatments

The order T3 > T1 > T2 is consistent with the proposed treatment mechanisms. APTES can, after hydrolysis and condensation, provide an aminofunctional surface capable of reacting with isocyanate groups [20]. The combination of higher strength, higher apparent modulus, and lower 24 h water absorption in T3 is compatible with improved interfacial interaction, but covalent bonding was not verified by spectroscopy and should therefore be regarded as a hypothesis rather than a demonstrated mechanism.

The NaOH treatment may partially remove surface lipids and increase roughness and wetting [15, [16]. Its intermediate performance is compatible with improved mechanical interlocking without severe keratin degradation, although neither surface morphology nor single-fiber strength was measured in this study.

The H_2O_2-treated series showed the smallest tensile-strength gain and the highest 24 h water absorption. Increased surface polarity after oxidation [17] offers a plausible explanation for the uptake result, but confirmation would require direct surface-energy and chemical analyses.

C. Porosity-Strength Relationship

The inverse ordering of mean estimated porosity and mean strength makes casting quality a potential alternative explanation for the treatment ranking. The ANCOVA provides useful evidence that series differences remain after adjustment for the available porosity proxy; however, the proxy is density-derived and is not equivalent to direct void-volume measurement.

The opposite signs of the pooled and within-series slopes illustrate an aggregation reversal. Because the within-series slopes are not individually significant and may reflect local fiber-content variation, they are not assigned a physical meaning. The defensible result is narrower: the treatment-series term remains large in the adjusted model, while true independence from casting porosity has not been demonstrated.

Surface treatment may influence wetting, air entrainment, and residual moisture, so interfacial state and casting quality can change together. Direct void characterization or a vacuum-cast replication would be needed to quantify their separate contributions.

A second limitation is the use of one fiber content. The present adjustment cannot establish whether the same ranking would persist at higher loadings, where dispersion and void formation may change.

D. Strength and Water Absorption do not Optimize Together

Relative to T0, T2 increased tensile strength by 1.22 MPa but also increased 24 h water absorption by 0.63 percentage points. T3 increased strength by 4.40 MPa and reduced 24 h uptake by 0.44 percentage points. Thus, among the tested composites, T3 provided the most favorable combination of these two measured responses. Application-specific durability still requires longer conditioning and post-exposure mechanical testing.

Within this dataset, T3 had the highest tensile strength, highest apparent modulus, highest apparent elongation, and lowest 24 h water absorption among the four reinforced series. Figure **6** summarizes this multivariate ranking. Because two deformation quantities are crosshead-based and moisture exposure lasted only 24 h, the plot is a comparison of measured laboratory responses rather than a general material-selection or ecodesign assessment.

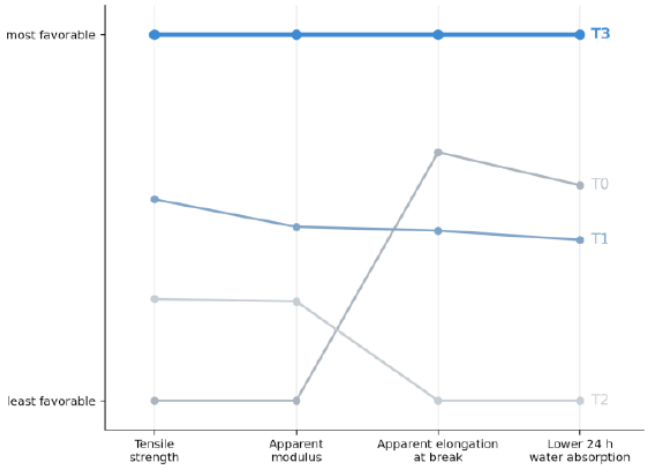

Figure 6: Normalized comparison of the four reinforced series for the measured laboratory responses. Higher normalized values indicate a more favorable value for the plotted criterion; the plot does not include long-term durability or environmental-impact metrics.

Table 13: Comparison with Published Results for Natural Fiber Composites

Source	System (neat matrix strength; fiber, content)	Treatment	Effect on tensile strength
This work	Rigid cast PUR, 32.66 MPa; wool, 10 wt%	washed only	−20.4% vs neat matrix
This work	idem	NaOH 0.1 M	+9.3% vs untreated fiber
This work	idem	H_2O_2 6%	+4.7% vs untreated fiber
This work	idem	APTES 1% v/v	+16.9% vs untreated fiber
[25]	Epoxy, 24–25 MPa; wool, 1.5–3 wt%	washed only	−8 to −17.5% vs neat matrix
[23]	Polypropylene and polyester; wool (review)	various	modulus raised, tensile strength impaired
[37]	Polyester; wool + date palm, 20 wt%	none	27 MPa absolute
[39]	Biobased PUR, 6.46 MPa; sisal	NaOH 10%	+118% vs neat matrix
[30]	PLA; hemp, 30 wt%	NaOH; NaOH + silane	+14%; +29% vs untreated fiber
[28]	TPU; sugar palm, 30 wt%	NaOH 2, 4, 6%	flexural +186% at 2%, falling above
[29]	Polyester; jute, 24–27 vol%	NaOH 2%, H_2O_2 30%	no significant tensile change
[31]	Natural fiber composites (review)	—	WA_{24} 0.7–2%; up to −40% after moisture exposure

Percentages are quoted against the reference stated in the same row, either the neat matrix or the untreated-fiber composite.

E. Comparison with published results

Published natural-fiber composites show both increases and decreases in tensile strength because the outcome depends on matrix properties, fiber type and content, orientation, processing, and interface quality. Table **13** places the present results beside the closest available comparisons; the different systems prevent direct quantitative equivalence.

Matrix strength and failure strain are important contributors to the sign of the reinforcement effect, but they are not the only controlling variables. In the present rigid polyurethane, wool increased apparent stiffness while reducing strength, consistent with published qualitative trends for wool composites [23]. Comparisons with epoxy, polyester, and biobased polyurethane systems should be interpreted as contextual rather than mechanistically conclusive because fiber content and processing differ [25, 37, 39].

The larger strength loss observed here at 10 wt% than in some lower-wool-content epoxy systems is compatible with a fiber-content effect, but the available cross-study data do not isolate fiber content from matrix and processing differences.

The higher performance of APTES relative to NaOH in the present system is qualitatively consistent with reports on silane-treated cellulosic composites [30]. This agreement supports, but does not prove, the proposed coupling interpretation for keratin-polyurethane interfaces.

The modest tensile benefit of H_2O_2 is consistent with literature showing that oxidative treatment can improve wetting without necessarily increasing tensile properties [29]. Direct transfer of that mechanism from jute-polyester to wool-polyurethane remains tentative.

Only one NaOH concentration and exposure time were tested, so no optimum can be identified. The selected mild condition produced a measurable gain relative to T0 without evidence in the composite data of a large performance penalty, but fiber-level degradation was not assessed.

The 24 h water-absorption values fall near the range summarized for natural-fiber composites [31], with T2 at the upper end. These measurements establish short-term uptake differences only; long-term conditioning and mechanical retesting are required before making claims about moisture resistance.

F. Limitations

The study has several limitations. Fiber orientation was neither controlled nor measured directly; the Krenchel calculation provides only an indirect indication. Only one fiber content and one condition per treatment were tested. Surface grafting, roughness, wetting, and fiber integrity were not characterized independently, so the proposed chemical mechanisms remain interpretations. Porosity was estimated from density rather than measured directly and can be influenced by local fiber content. Strain was obtained from crosshead displacement, making modulus and elongation apparent quantities that include machine and grip compliance. The 0.1% elongation resolution limits small comparisons, and the single wool lot and single processing campaign do not establish between-lot or production-scale reproducibility. Finally, the 24 h immersion test does not establish long-term moisture resistance, and no life-cycle assessment was performed to quantify an ecodesign benefit.

6. CONCLUSIONS

This study compared untreated, NaOH-treated, H_2O_2-treated, and APTES-treated sheep wool fibers at 10 wt% in the same rigid cast polyurethane, using twenty tensile specimens per series.

Adding washed wool reduced mean tensile strength from 32.66 to 26.00 MPa and increased the crosshead-based apparent modulus from 727 to 793 MPa. All three treatments increased strength relative to untreated wool, with the order APTES > NaOH > H_2O_2. APTES reached 30.40 MPa, 16.9% above T0 but 6.9% below the neat matrix, and also gave the lowest 24 h water absorption among the reinforced series. Accordingly, APTES was the best-performing treatment under the specific formulation and processing conditions tested; the result is comparative and does not establish an optimized treatment condition.

Calculations based on literature fiber properties and assumed interfacial shear strength placed the critical length between 0.21 and 1.43 mm, below the nominal 10 mm fiber length. A Krenchel-type analysis produced apparent efficiency factors consistent with preferential alignment, but neither fiber orientation nor interfacial shear strength was measured directly. These calculations should therefore be treated as supporting interpretations rather than independent experimental findings.

Mean density-derived porosity decreased in the same order that tensile strength increased. In an exploratory ANCOVA, the series effect remained significant after adjustment for this porosity proxy. This supports the robustness of the observed treatment ranking within the dataset, but it does not prove independence from true void content because porosity was not measured directly.

Future work should directly quantify void content, verify surface modification by spectroscopy and wettability measurements, measure fiber orientation and single-fiber properties, use an extensometer for strain, test several fiber contents and treatment conditions, and evaluate mechanical-property retention after longer moisture conditioning.

The results demonstrate a promising route for valorizing coarse sheep wool in rigid polyurethane composites, while also showing that the neat-matrix tensile strength was not fully recovered. Claims regarding long-term durability, environmental benefit, or a specific APTES bonding mechanism require dedicated measurements beyond the scope of the present study.

AUTHOR CONTRIBUTIONS

S.L, D.D., and F.C.C.: Conceptualization, Methodology, Writing—review & editing, Validation. S.L, D.D., A.S: and F.C.C., Visualization, Validation, Investigation. S.L, D.D., A.S: and F.C.C.: Methodology, Data curation, Validation, Resources, Writing—original draft, Software, Formal analysis. S.L, D.D., A.S: and F.C.C.: Project administration, Supervision. All authors have read and agreed to the published version of the manuscript.

CONFLICT OF INTEREST STATEMENT

The authors declare that they have no known competing financial interests or personal relationships that could have appeared to influence the work reported in this paper.

REFERENCES

[1] S. Lazăr, D. Dobrotă, R.-E. Breaz, and S.-G. Racz, "Eco-design of polymer matrix composite parts: A review," Polymers, vol. 15, no. 17, art. 3634, 2023. https://doi.org/10.3390/polym15173634

[2] T. Eleutério, M. J. Trota, M. G. Meirelles, and H. C. Vasconcelos, "A review of natural fibers: Classification, composition, extraction, treatments, and applications," Fibers, vol. 13, no. 9, art. 119, 2025. https://doi.org/10.3390/fib13090119

[3] M. Arya, M. Skrifvars, and P. Khalili, "Performance and life cycle assessment of composites reinforced with natural fibers and end-of-life textiles," J. Compos. Sci., vol. 8, no. 6, art. 196, 2024. https://doi.org/10.3390/jcs8060196

[4] M. B. Kulkarni, V. Gavande, P. A. Mahanwar, A. R. Shah, R. K. Shuib, A. M. Khare, and S. Radhakrishnan, "Review on biomass sheep wool-based polymer composites," Biomass Convers. Biorefin., vol. 14, no. 24, pp. 30961–30982, 2024. https://doi.org/10.1007/s13399-023-04912-4

[5] J. Szczecina, E. Szczepanik, J. Barwinek, P. Szatkowski, M. Niemiec, A. I. Zhakypbekovich, and E. Molik, "Sheep wool as biomass: Identifying the material and its reclassification from waste to resource," Energies, vol. 18, no. 19, art. 5185, 2025. https://doi.org/10.3390/en18195185

[6] D. Jóźwiak-Niedźwiedzka and A. P. Fantilli, "Wool-reinforced cement based composites," Materials, vol. 13, no. 16, art. 3590, 2020. https://doi.org/10.3390/ma13163590

[7] S. Jose, S. Boruah, and S. Rani, "Wool-polymer composites: A comprehensive review on preparation, properties, and applications," J. Nat. Fibers, vol. 22, no. 1, art. 2495921, 2025. https://doi.org/10.1080/15440478.2025.2495921

[8] C. Ruiz-Díaz, Ó. Rodríguez-Alabanda, M. M. Serrano-Baena, and G. Guerrero-Vacas, "Recent advances in biocomposite materials reinforced with raw or minimally processed wool: Fabrication methods, properties and applications—A systematic review," J. Compos. Sci., vol. 10, no. 2, art. 104, 2026. https://doi.org/10.3390/jcs10020104

[9] A. Shavandi and M. A. Ali, "Keratin based thermoplastic biocomposites: A review," Rev. Environ. Sci. Biotechnol., vol. 18, pp. 299–316, 2019. https://doi.org/10.1007/s11157-019-09497-x

[10] O. Starkova, A. Sabalina, V. Voikiva, and A. Osite, "Environmental effects on strength and failure strain distributions of sheep wool fibers," Polymers, vol. 14, no. 13, art. 2651, 2022. https://doi.org/10.3390/polym14132651

[11] J. Braniša, K. Koóšová, and M. Porubská, "Selective modifications of sheep wool usable in non-textile applications," Polymers, vol. 16, no. 10, art. 1380, 2024. https://doi.org/10.3390/polym16101380

[12] A. Olszewski, P. Kosmela, A. Mielewczyk-Gryń, and Ł. Piszczyk, "Bio-based polyurethane composites and hybrid composites containing a new type of bio-polyol and addition of natural and synthetic fibers," Materials, vol. 13, no. 9, art. 2028, 2020. https://doi.org/10.3390/ma13092028

[13] X. Yuan, S. Fu, and H. Liu, "Preparation of wood fiber-polyurethane plastic composite with water resistance and high strength," Materials, vol. 18, no. 6, art. 1314, 2025. https://doi.org/10.3390/ma18061314

[14] K. Kamińska, M. Barczewski, M. Kurańska, E. Malewska, K. Polaczek, and A. Prociak, "The effect of a chemical foaming agent and the isocyanate index on the properties of open-cell polyurethane foams," Materials, vol. 15, no. 17, art. 6087, 2022. https://doi.org/10.3390/ma15176087

[15] D. Verma and K. L. Goh, "Effect of mercerization/alkali surface treatment of natural fibres and their utilization in polymer composites: Mechanical and morphological studies," J. Compos. Sci., vol. 5, no. 7, art. 175, 2021. https://doi.org/10.3390/jcs5070175

[16] M. Aravindh, S. Sathish, R. Ranga Raj, A. Karthick, V. Mohanavel, P. P. Patil, M. Muhibbullah, and S. M. Osman, "A review on the effect of various chemical treatments on the mechanical properties of renewable fiber-reinforced composites," Adv. Mater. Sci. Eng., vol. 2022, art. 2009691, pp. 1–24, 2022. https://doi.org/10.1155/2022/2009691

[17] X. Wang, X. Shen, and W. Xu, "Effect of hydrogen peroxide treatment on the properties of wool fabric," Appl. Surf. Sci., vol. 258, no. 24, pp. 10012–10016, 2012. https://doi.org/10.1016/j.apsusc.2012.06.065

[18] L. Conzatti, F. Giunco, P. Stagnaro, A. Patrucco, C. Tonin, C. Marano, M. Rink, and E. Marsano, "Wool fibres functionalised with a silane-based coupling agent for reinforced polypropylene composites," Compos. Part A Appl. Sci. Manuf., vol. 61, pp. 51–59, 2014. https://doi.org/10.1016/j.compositesa.2014.02.005

[19] F. Pawlak, M. Aldas, F. Parres, J. López-Martínez, and M. P. Arrieta, "Silane-functionalized sheep wool fibers from dairy industry waste for the development of plasticized PLA composites with maleinized linseed oil for injection-molded parts," Polymers, vol. 12, no. 11, art. 2523, 2020. https://doi.org/10.3390/polym12112523

[20] Y. Xie, C. A. S. Hill, Z. Xiao, H. Militz, and C. Mai, "Silane coupling agents used for natural fiber/polymer composites: A review," Compos. Part A Appl. Sci. Manuf., vol. 41, no. 7, pp.

806–819, 2010.
https://doi.org/10.1016/j.compositesa.2010.03.005

[21] E. C. Șchiopu, S. Lazăr, D. Dobrotă, N. F. Cofaru, and N.-Ș. Drăgan, "Interlocking geometric interfaces for functionally-adapted localized reinforcement in polymer matrix composites: Parametric FEA design rules and experimental validation," J. Mater. Res. Technol., vol. 43, pp. 760–788, 2026.
https://doi.org/10.1016/j.jmrt.2026.06.084

[22] S. Tiwari, J. Lee, M. F. Khan, and N. Park, "Statistical variability and lower-tail performance assessment of tensile properties in flax, jute, and carbon fiber composite laminates," Polymers, vol. 18, no. 14, art. 1746, 2026.
https://doi.org/10.3390/polym18141746

[23] A. Patrucco, M. Zoccola, and A. Anceschi, "Exploring the potential applications of wool fibers in composite materials: A review," Polymers, vol. 16, no. 16, art. 2360, 2024.
https://doi.org/10.3390/polym16162360

[24] A. Mishra, N. K. Kim, and D. Bhattacharyya, "Keratinous natural fibres as sustainable flame retardants and reinforcements in polymer composites," J. Compos. Sci., vol. 8, no. 6, art. 230, 2024.
https://doi.org/10.3390/jcs8060230

[25] C. Ruiz-Díaz, G. Guerrero-Vacas, and Ó. Rodríguez-Alabanda, "Mechanical performance of wool-reinforced epoxy composites: Tensile, flexural, compressive, and impact analysis," Materials, vol. 18, no. 23, art. 5391, 2025.
https://doi.org/10.3390/ma18235391

[26] S. Mattiello, A. Guzzini, A. Del Giudice, C. Santulli, M. Antonini, G. Lupidi, and R. Gunnella, "Physico-chemical characterization of keratin from wool and chicken feathers extracted using refined chemical methods," Polymers, vol. 15, no. 1, art. 181, 2023.
https://doi.org/10.3390/polym15010181

[27] F. C. da Silva, H. P. Felgueiras, R. Ladchumananandasivam, J. U. L. Mendes, K. K. O. S. Silva, and A. Zille, "Dog wool microparticles/polyurethane composite for thermal insulation," Polymers, vol. 12, no. 5, art. 1098, 2020.
https://doi.org/10.3390/polym12051098

[28] D. Bachtiar, A. A. Mohammed, S. Palanisamy, A. I. Imran, J. P. Siregar, M. R. M. Rejab, Syaubari, T. Cionita, D. F. Fitriyana, S. A. Al-Farraj, M. I. Almansour, and Q. Ma, "Effect of alkaline treatment on the thermal and mechanical properties of sugar palm fibre reinforced thermoplastic polyurethane composites," Sci. Rep., vol. 15, art. 14085, 2025.
https://doi.org/10.1038/s41598-025-99227-x

[29] A. L. L. Flores, A. Kairytė, J. Šeputytė-Jucikė, S. Makowska, A. Lavoratti, R. de Avila Delucis, and S. C. Amico, "Effect of chemical treatments on the mechanical properties of jute/polyester composites," Materials, vol. 17, no. 10, art. 2320, 2024.
https://doi.org/10.3390/ma17102320

[30] P. F. Alao, L. Marrot, M. D. Burnard, G. Lavrič, M. Saarna, and J. Kers, "Impact of alkali and silane treatment on hemp/PLA composites¥u2019 performance: From micro to macro scale," Polymers, vol. 13, no. 6, art. 851, 2021, doi: 10.3390/polym13060851.
https://doi.org/10.3390/polym13060851

[31] A. Pavlovic, L. Valzania, and G. Minak, "Effects of moisture absorption on the mechanical and fatigue properties of natural fiber composites: A review," Polymers, vol. 17, no. 14, art. 1996, 2025,
https://doi.org/10.3390/polym17141996

[32] Altropol Kunststoff GmbH, "NEUKADUR MultiCast 1 — 2-C PUR fast cast system," product technical data sheet, Stockelsdorf, Germany. [Online]. Available: https://www.altropol.de/en/products/product-groups/neukadur-polyurethane-systems

[33] ASTM D638-22, Standard Test Method for Tensile Properties of Plastics, ASTM International, West Conshohocken, PA, USA, 2022.

[34] ASTM D792-20, Standard Test Methods for Density and Specific Gravity (Relative Density) of Plastics by Displacement, ASTM International, West Conshohocken, PA, USA, 2020.

[35] ASTM D2240-15(2021), Standard Test Method for Rubber Property—Durometer Hardness, ASTM International, West Conshohocken, PA, USA, 2021.

[36] ASTM D570-22, Standard Test Method for Water Absorption of Plastics, ASTM International, West Conshohocken, PA, USA, 2022.

[37] A. F. Mohamed, M. Y. Abdellah, A. H. Backar, M. K. Hassan, M. Kourmpetis, and A. Mellouli, "Multi-objective optimization and reliability assessment of date palm fiber/sheep wool hybrid polyester composites using RSM and Weibull analysis," Polymers, vol. 17, no. 20, art. 2786, 2025.
https://doi.org/10.3390/polym17202786

[38] R. Żurawik, J. Volke, J.-C. Zarges, and H.-P. Heim, "Comparison of real and simulated fiber orientations in injection molded short glass fiber reinforced polyamide by X-ray microtomography," Polymers, vol. 14, no. 1, art. 29, 2022.
https://doi.org/10.3390/polym14010029

[39] B. T. Oliveira and R. M. Parreira, "Mechanical performance of biobased polyurethane composites reinforced with treated sisal fibers," Polímeros, vol. 36, no. 1, art. e20260004, 2026.
https://doi.org/10.1590/0104-1428.20250057

https://doi.org/10.12974/2311-8717.2026.14.11